Available online at www.sciencedirect.com
SCIENCE DIRECT®
International Journal of Mass Spectrometry 232 (2004) 99–105
International Journal of Mass Spectrometry
www.elsevier.com/locate/ijms

Electron impact ionization of 5- and 6-chlorouracil: appearance energies

S. Denifl, S. Ptasińska, B. Gstir, P. Scheier, T.D. Märk*

Institut für Ionenphysik, Leopold-Franzens Universität, Technikerstrasse 25, A-6020 Innsbruck, Austria

Received 13 October 2003; accepted 25 November 2003

Abstract

Electron impact ionization of the gas phase modified DNA/RNA bases 5- and 6-ClU was studied using a crossed electron/neutral beams technique in combination with a quadrupole mass spectrometer. 5- and 6-ClU belong to the class of halouracils which are used in radiation therapy to increase the effect of ionizing radiation to tumours, when they are incorporated into cancer tissue. Besides determining the mass spectra for both molecules at the electron energy of 70 eV, the ionization efficiency curves for each parent ion and the most abundant fragment ions were measured near the threshold and the corresponding appearance energies (AEs) were derived using an iterative, non-linear least square fitting procedure using the Marquart–Levenberg algorithm based on the Wannier threshold law. The most abundant cations observed in mass spectra have a threshold value of AE $((C_3H_2ClNO)^+/5\text{-ClU}) = 11.12 \pm 0.03$ eV and AE $((C_3H_2NO)^+/6\text{-ClU}) = 12.06 \pm 0.03$ eV. The present AE value for the parent ion of 5-ClU AE$((5\text{-ClU})^+/5\text{-ClU}) = 9.38 \pm 0.05$ eV is in fair agreement with previous calculations at the B3LYP level of theory. The AE$((6\text{-ClU})^+/6\text{-ClU}) = 9.71 \pm 0.05$ eV is 0.33 eV higher than that for 5-ClU.

Keywords: Electron impact ionization; 5- and 6-CIU; Mass spectra; Appearance energies

1. Introduction

The lethal effect of radiation damage for cells is sometimes unwanted like in the case of radioactivity, but it is also desirable as in the case of radiation therapy. One problem in medicine is that only the cancerous cell material should be destroyed, but healthy tissue should stay unaffected. One way to control this damage is the application of radio sensitizers [1,2] that are incorporated into cancer cells. Cancer tissues doped with these sensitizer molecules will be destroyed preferentially under radiation exposure, at radiation doses which are low enough that healthy cell material is unaffected. With this method unwanted side effects for patients can be decreased.

Generally the genotoxic effect of high energy radiation (α, β, γ and heavy ions) with living cells is not only caused by the direct impact of the primary high energy projectiles, but primary particles remove secondary electrons from the molecules along the track and due to subsequent charge transfer and energy dissipating processes neutral or ionic radicals are formed. One third of the damage to the genom due to ionizing radiation is direct, that means energy is deposited into the DNA and its closely bound water molecules [3]. Two third of the damage is caused indirectly by free radicals that are formed close to the DNA in water molecules and other bio molecules. The most important radical for indirect damage is the very reactive hydroxyl radical [4]. The activity of this radical has been also observed in experiments of low energy photons with dry or hydrated DNA [5] resulting in an increase of DNA strand breaks. Secondary electrons that are created due to the primary particles are produced in large amounts (4×10^4 electrons per 1 MeV deposited primary quantum energy [6]) with initial kinetic energies up to about 20 eV [7]. In subsequent inelastic collisions with the medium they are thermalized within 10^{-12} s before they become inactive because they reach the stage of solvation. As shown recently by Sanche and co-workers [8] such free secondary electrons in a low energy range near and also below the ionization limit are able to induce damage in super coiled DNA like single and double strand breaks. Additionally there exists a variety of experiments concerning electron attachment [9,10] and electron ionization [11,12] of isolated gas phase DNA and RNA components to study the intrinsic behaviour of these molecules during interaction with free electrons.

These experiments [8–12] were performed with unmodified DNA and RNA molecules. We started recently inves-

* Corresponding author. Adjunct professor at Department of Plasmaphysics, Comenius University, SK-84248 Bratislava, Slovak Republic.
E-mail address: tilmann.maerk@uibk.ac.at (T.D. Märk).

1387-3806/$ – see front matter © 2003 Elsevier B.V. All rights reserved.
doi:10.1016/j.ijms.2003.11.010

tigations concerning the interaction between electrons and isolated modified molecules in order to investigate differences in their intrinsic behaviour. This may give new insight into the increased sensitivity of radiosensitizers. One possible class of radio-sensitizers are halouracils (5- and 6-XU, respectively) (X = F, Cl, Br and I), which belong to the group of substituted pyrimidines. The 5-XUs can be substituted for thymine (T) in DNA and for uracil (U) in RNA leading to an increased sensitivity of cells to ionizing radiation [1]. The underlying mechanism of the enhancement of sensitivity to radiation damage is still a matter of investigations. Recent studies showed that low energy electrons in a range from 0 to 3 eV effectively dissociate XUs [13–17]. The main products are X^- and $(XU\text{-}X)^-$ together with the complementary neutrals exhibiting cross sections which are one to two orders of magnitude larger than cross sections reported for the anions formed in attachment to thymine or uracil [9,10]. The conclusion was that part of the increased sensitivity is connected to the increased efficiency for resonant low energy electron attachment processes which lead to the formation of various genotoxic radicals. Nevertheless it is important to study in addition the positive ion formation near the ionization limit to investigate possible differences between XUs and unmodified DNA and RNA molecules as these differences may also contribute to the increased sensitivity of substituted pyrimidines.

In this work, we present a detailed experimental study of electron impact ionization of 5- and 6-ClU (see Fig. 1 showing the molecular structures) near the ionization threshold. In addition, we measured mass spectra to study the fragmentation patterns of both molecules at electron impact energy of 70 eV. From these results, we may collect additional information for the increased sensitivity of halouracils in interaction with ionizing radiation. To our best knowledge, there exists no previous experimental determination of appearance energies of 5- and 6-chlorouracil and their fragmentation products. Nevertheless there exist theoretical studies by Wetmore et al. [18] concerning the determination of ionization energies (IE) and electron affinities (EA) of 5-halouracils. They performed calculations at the B3LYP level of theory using the Gaussian 98 program. They compared their results with a previous calculation [19] where they determined IEs and EAs of unmodified DNA and RNA molecules. From the calculations of adiabatic and vertical IEs and EAs for all DNA bases, uracil and all 5-XUs in gas phase and solution they concluded that their results confirm the assumption that 5-XUs enhance the sensitivity of ionizing radiation of DNA. In their opinion the major mechanism of enhanced DNA or RNA damage involves the formation of anions which dissociate into further anions plus radicals causing even more damage. In the case of positive ion formation they observed a small decrease of the IE for halouracils in comparison to uracil and because of this they expect that XUs are also more active to form cationic sites.

2. Experimental setup

The apparatus used in the present experimental investigation is a hemispherical electron monochromator in conjunction with a quadrupole mass spectrometer. A detailed description can be found in [20]. Electrons are emitted from a hairpin filament with typical resolution of 1 eV and focussed with a lens system into the entrance slit of a custom made 180° hemispherical analyser. This allows reducing the spread of the kinetic energy of the electron beam to a best value of about 35 meV [21]. In the present studies an electron energy resolution of approximately 100 meV was used resulting in a higher yield of the formed cations than using the 35 meV resolution. After the analyzer, the monochromatized electrons are focussed and accelerated with a second lens system into the collision chamber, where the interaction with the neutral beam takes places. The standard electron energy range is from about 0 to 100 eV, with additional power supplies a maximum electron energy of 600 eV can be reached. After the collision chamber the electron beam is collected at a final plate, where the electron current is measured. These measurements were performed with an electron current of 5–8 nA. The neutral beam is generated by heating chlorouracil (purity 99%, from Sigma-Aldrich) in a Knusden type oven. The temperature of the oven during the experiments was 180 and 160 °C in the case of 5- and 6-ClU, respectively, which was measured with a Pt100 resistance temperature sensor mounted at the oven. For increasing the

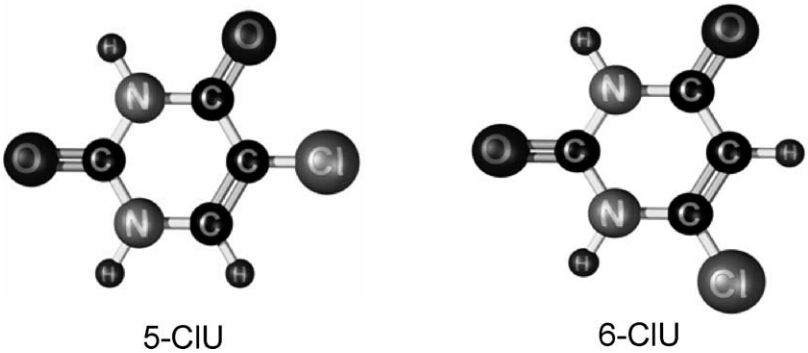

Fig. 1. Molecular structure of 5- and 6-ClU, respectively.

neutral beam intensity a capillary (length 8 cm) was added to the oven. With this setup the neutral molecules then effuse directly into the collision chamber through a hole with a diameter of 1 mm. Ions formed in the collision chamber after electron impact are then extracted by a weak field (at maximum 200 meV/cm) into the entrance of a quadrupole mass spectrometer with a mass range of 2048 amu. The flight time of the ions from the center of the collision chamber to the entrance of the quadrupole is between 15 and 35 μs depending on the mass. The mass analysed ions are detected by a channeltron type SEM operated in a pulse counting mode and recorded by a computer. In the present work the ionization efficiency curves were measured as a function of the electron energy in a range from about 5 eV below the threshold to 5 eV above its onset. The energy scale was calibrated with the well known value of the appearance energy of krypton [12] measured under the same experimental conditions.

3. Data analysis

To determine an accurate value of the appearance energy (AE) for cations we perform a fitting procedure which is described in detail in Ref. [22]. In short, we use a fitting routine using the Marquart–Levenberg algorithm, which derives a non-linear weighted least squares fit of the raw data. The fitting procedure is based on a Wannier type threshold law, where a fitting function $f(E)$ is fitted over the energy range that includes the threshold region:

$$f(E) = b, \quad \text{if the incident electron energy } E < \text{AE} \tag{1a}$$

$$f(E) = b + c(E - \text{AE})^p, \quad \text{if the incident electron energy } E > \text{AE} \tag{1b}$$

The fit involves then four parameters: the background signal b, the appearance energy AE, which should be determined, a scaling constant c which determines the slope of the cross section above the AE and finally an exponential factor p (Wannier factor).

A 2-function fit is used in cases, where the background signal is constant as a function of the electron energy. In more involved cases, where the background signal is no longer constant, it is necessary to use a 3-function fitting method. This procedure is also used when the ionization yield exhibits besides a first onset a change in slope at a higher electron energy corresponding to a second appearance energy. The fit has the following form:

$$f(E) = b, \quad \text{if } E < \text{AE}_1 \tag{2a}$$

$$f(E) = b + c(E - \text{AE}_1)^{p_1}, \quad \text{if } \text{AE}_1 < E < \text{AE}_2 \tag{2b}$$

$$f(E) = b + c(E - \text{AE}_1)^{p_1} + d(E - \text{AE}_2)^{p_2}, \quad \text{if } E > \text{AE}_2 \tag{2c}$$

AE_1 is the appearance energy of the first threshold whereas AE_2 corresponds to the second onset.

Using the SIGMAPLOT program, the fitting procedure calculates the four fitting parameters in the case of fitting function (1) and the corresponding standard deviations. In the case of two thresholds, the fit function (2) was used employing the ORIGIN program. The data were fitted over an energy range from a few electron volts below the threshold to about 3 eV above its onset (for details, see Ref. [20]). With this fitting method, we determined the AEs of some rare gases (Ar, Kr, Xe) and of some simple molecules (N_2, O_2, N_2O) to test the accuracy of the fitting and the linearity of the energy scale [23]. Excellent agreement (within 10 meV) was found with spectroscopical values (which are listed in NIST database [12]). One can conclude that this is an exact and reliable method to determine AEs of atoms or molecules. Recently with this experimental setup and fitting procedure the AEs of fluorinated hydrocarbons, propane and methane [24] and compounds of atmospheric relevance such as Cl_2O [25] and SF_5CF_3 [26] were derived. Beside that also the isotopic shift for hydrogen, water and benzene molecules was determined [27]. Recently it was also possible to quantify temperature effects in appearance energies [28]. For complex molecules often the experimentally determined appearance energies of fragment ions depend strongly on the time scale of the instrument. A distribution of the excitation energy into the internal degrees of freedom and a statistical accumulation of this energy into a specific bond that will finally lead to the dissociation of the ion require a surplus of energy to observe a fragment ion at a specific time after the ionization event. For instance in the case of C_{60} the so called kinetic shift for the detection of the fragment C_{58}^+ 10 μs after the electron impact is 35 eV [29].

4. Results and discussion

4.1. Mass spectra

Fig. 2 shows the mass spectrum of 5-ClU ($C_4H_3ClN_2O_2$) measured at an electron energy of 70 eV. The peaks between 146 and 149 amu can be clearly identified as being due to the parent ion and the corresponding isotopes due to the ^{13}C (abundance 1.11%) and ^{37}Cl (24.47%) isotope. The isotope abundance also leads to possible structure of fragment ion peaks, which facilitates identifying the fragments ions. The ion with the highest intensity in this mass spectrum is at mass 103 amu which can be identified as $(C_3H_2ClNO)^+$. This ion is formed by loss of CNOH. The second highest abundance exhibits $(C_2HClO)^+$ at mass 76 amu. Another possible fragment ion appearing at this mass would be $(C_4N_2)^+$, but the peak at mass 78 amu indicates the presence of an isotope peak of a fragment ion including a chlorine atom. In the mass region below 70 amu, the fragment ions with the highest abundance are at mass 60 amu $(C_2HCl)^+$, 48 amu $(CHCl)^+$, and 28 amu $(CO)^+$. In the NIST database [12], there exists

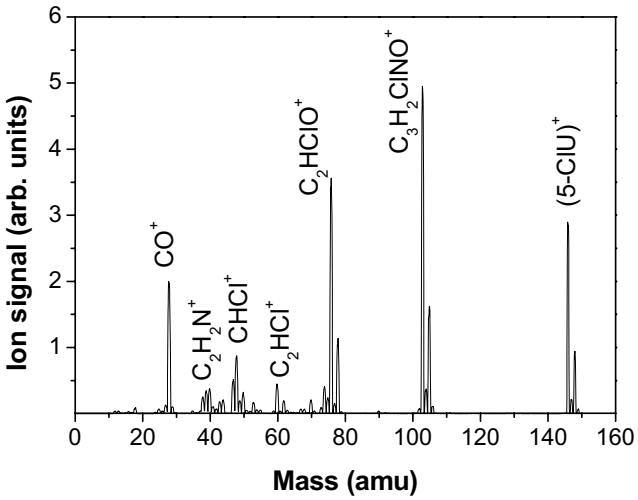

Fig. 2. Mass spectrum obtained by electron impact ionization of 5-chloruracil at an electron energy of 70 eV.

no mass spectrum of 5-ClU, but it contains a mass spectrum of uracil, where a hydrogen atom sits instead of the chlorine atom at the 5-C atom. With the present setup, we also determined a mass spectrum of uracil [11] which is in good agreement with the NIST spectrum. In both cases, the production of a parent ion and the formation of an ion which is formed by subtraction of a CNOH group (mass 69 amu in the case of uracil and mass 103 amu in 5-ClU) is observed. Also the formation of a fragment ion 70 amu below the parent ion is visible in both mass spectra (mass 42 amu in uracil and 76 amu in 5-ClU).

Fig. 3 shows the mass spectrum of 6-ClU again determined at an electron energy of 70 eV. Besides the production of a parent cation one of the most abundant fragment ion can be also found at mass 103 amu. One difference is that the peak at mass 111 that is associated with $((6\text{-ClU})\text{-Cl})^+$ is approximately 100 times higher than in the case of 5-ClU.

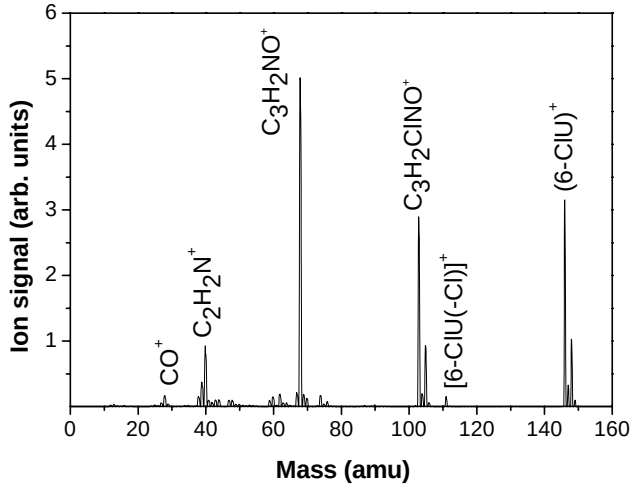

Fig. 3. Mass spectrum of 6-chlorouracil produced by 70 eV electron impact on neutral 6-chlorouracil.

Another major difference is the absence of the second most abundant peak of the 5-ClU spectrum at mass 76 amu. Instead of this the most abundant fragment ion can be found at mass 68 amu, which can be identified as $(C_3H_2NO)^+$. Below 65 amu, the fragmentation pattern is very similar to 5-ClU although the abundance for fragment ions is different, e.g. the $(CO)^+$ peak (28 amu) is much less abundant in the mass spectrum of 6-ClU. In contrary to 5-ClU there exists a mass spectrum of 6-ClU in the NIST database [12] which was measured at an electron energy of 70 eV. There is agreement with this NIST spectrum concerning the formation of fragment ions although the abundance of ions is different. In the NIST spectrum, masses higher than 80 amu seem to be less abundant than in the present mass spectrum. This can be explained with different ion extraction and detection efficiencies of the experimental setup used for the NIST-mass spectrum and the present setup.

4.2. Appearance energies

For the most abundant cations we measured for both molecules the ionization efficiency yields near the threshold. Fig. 4 shows the ionization efficiency curves for the parent ion and seven fragment ions of 5-ClU. The experimental data were fitted with the method described above. The AEs determined for 5-ClU are listed in Table 1. The AEs given in Table 1 are the mean values of several data sets whereas the AEs given in Fig. 4 show individual values. The parent ion exhibits with a value of 9.38 ± 0.05 eV, the lowest threshold of all measured ionization efficiency curves. The most abundant fragment ion in the 5-ClU mass spectrum $(C_3H_2ClNO)^+$ has an AE of 11.12 ± 0.03 eV; that is the second lowest AE of all AEs determined in this work. A significantly higher AE has the cation $(C_2HClO)^+$ (mass 76 amu), which is the second highest in abundance in 5-ClU mass spectrum. The cation at mass 40 amu $(C_2H_2N)^+$ has a second onset; so the measured cross section was analysed using the fit procedure which allows for two thresholds. The first onset is very likely due to ionization of pump oils present as background in the chamber that appears at this mass and only the second threshold is the AE for the formation of $((C_2H_2N)^+/5\text{-ClU})$. The ion at mass 28 amu identified as $(CO)^+$ has an AE value of 13.96 ± 0.05 eV.

Table 1
AE for cations of 5-ClU produced by electron impact on neutral 5-ClU

Cation produced by electron impact of 5-ClU	Mass (amu)	Present AE value (eV)
$(5\text{-ClU})^+$	146	9.38 ± 0.05
$(C_3H_2ClNO)^+$	103	11.12 ± 0.03
$(C_2HClO)^+$	76	13.19 ± 0.03
$(C_2HCl)^+$	60	13.97 ± 0.06
$(CHCl)^+$	48	14.92 ± 0.07
$(CCl)^+$	47	16.8 ± 0.4
$(C_2H_2N)^+$	40	12.34 ± 0.2, 16.08 ± 0.2
$(C_2HN)^+$	39	15.61 ± 0.10
$(CO)^+$	28	13.96 ± 0.05

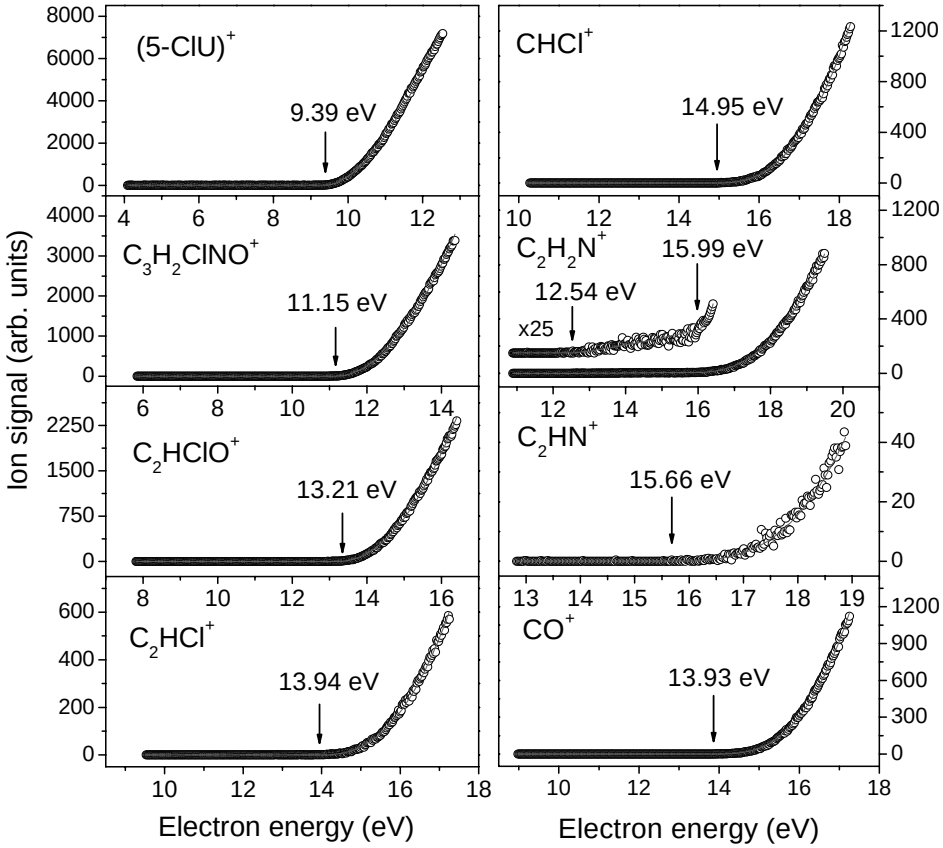

Fig. 4. Ionization efficiency curves near the threshold region for the formation of 5-ClU cations from neutral 5-ClU by electron impact. The energy scale was calibrated with krypton measured under the same conditions. The measured data are shown as open circles; the fit curves (derived by the fitting procedure described in text) are shown as solid lines. AEs, which are indicated by arrows, are the thresholds for these individual data sets and differ from the AEs given in the text and in Table 1 which were derived by averaging several values from different data sets.

Fig. 5 shows the ionization efficiency curves near the threshold for the parent ion 6-ClU and for 5 fragment ions with the highest abundance that have been observed in the 6-ClU mass spectrum. The determined AEs are listed in Table 2. The AE of 6-ClU$^+$ has a value of 9.71 ± 0.05 eV, which is 0.33 eV higher than that of 5-ClU. The AE of uracil (see Table 3) lies between the values of the two chlorouracils. The fragment ion at mass 111 amu that is associated with ((6-ClU)-Cl)$^+$ and the ion at mass 103 amu ((6-ClU)-(CHNO))$^+$ have very similar AEs, i.e., the AE of ((6-ClU)-(CHNO))$^+$ is 50 meV lower than that of ((6-ClU)-Cl)$^+$. Like for the parent ions of the two ClUs the AE for the fragment ion at mass 103 formed from neutral 6-ClU has a higher value than the one from 5-ClU, i.e., the observed difference to ((C_3H_2ClNO)$^+$/5-ClU) is 190 meV. The most abundant ion, which was observed in the 6-ClU mass spectrum, (C_3H_2NO)$^+$ (mass 68 amu) has a threshold value of 12.06 ± 0.03 eV. The ion yield at mass 40 amu shows two onsets like in the case of 5-ClU, where the first onset is attributed to the ionization threshold of pump oils, i.e., for both molecules the first AE has the same value within the error bar. The second thresh-

Table 2
AE for cations of 6-ClU produced by electron impact on neutral 6-ClU

Cation produced by electron impact of 6-ClU	Mass (amu)	Present AE value (eV)
(6-ClU)$^+$	146	9.71 ± 0.05
((6-ClU)-Cl)$^+$	111	11.36 ± 0.05
(C_3H_2ClNO)$^+$	103	11.31 ± 0.03
(C_3H_2NO)$^+$	68	12.06 ± 0.03
(C_2H_2N)$^+$	40	12.31 ± 0.25, 15.72 ± 0.25
(CO)$^+$	28	14.11 ± 0.18

Table 3
Comparison of the present AEs of parent cations (5-ClU)$^+$ and (6-ClU)$^+$ with calculated values by Wetmore et al. [18] and with previous experimentally determined AEs of thymine and uracil

Parent cation	Eperimental AE (in eV)	Calculated AE (in eV) [18]
5-ClU	9.38 ± 0.05	9.21
6-ClU	9.71 ± 0.05	–
Uracil	9.59 ± 0.06 [11]	9.47
Thymine	9.15 ± 0.15 [30]	9.02
5-BrU	–	9.07
5-FlU	–	9.46

Other experimental values for vertical ionization energies given in [12] for thymine range from 9.02 to 9.20 eV and in the case of uracil from 9.45 to 9.68 eV.

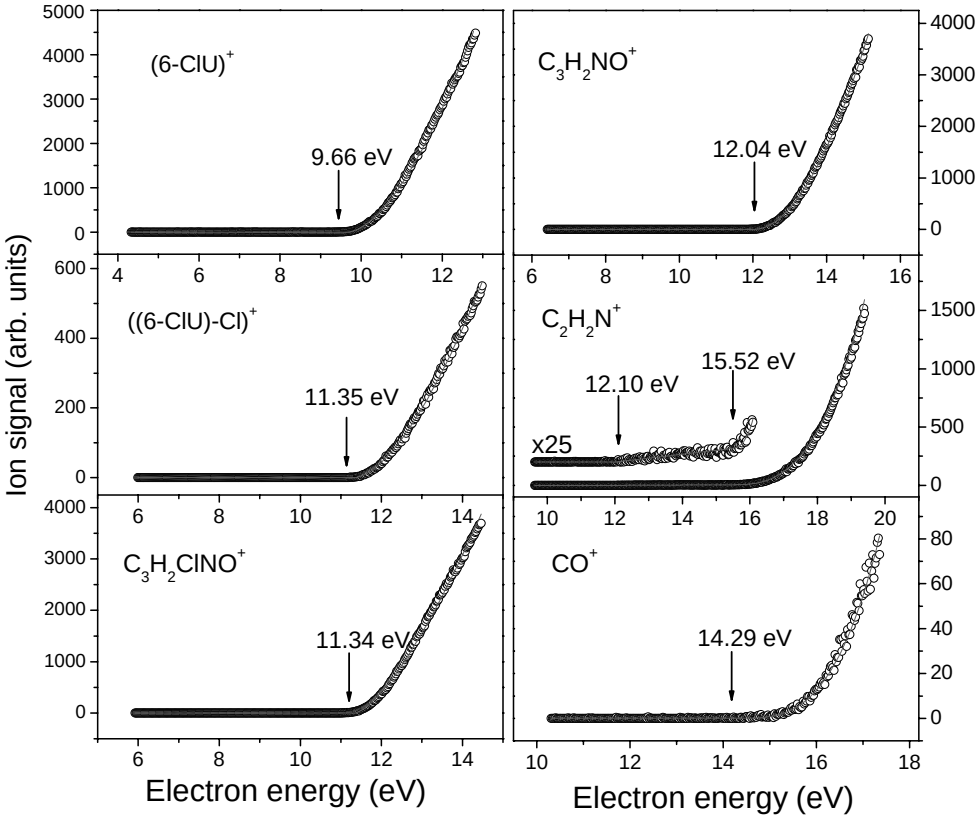

Fig. 5. Ionization efficiency curves near the threshold region for the formation of 6-ClU cations from neutral 6-ClU by electron impact. The energy scale was calibrated with krypton measured under the same conditions. The measured data are shown as open circles; the fit curves (derived by the fitting procedure described in text) are shown in solid lines. AEs, which are indicated by arrows, are the thresholds for these individual data sets and differ from the AEs given in text and in Table 2 which were derived by averaging several values from different data sets.

old for $((C_2H_2N)^+$/6-ClU) is 360 meV lower than that for $((C_2H_2N)^+$/5-ClU).

In Table 3, the present values are compared with experimentally determined values of AEs of uracil, thymine and with theoretical calculations by Wetmore et al. [18] concerning the vertical ionization energies of (modified) pyrimidines. The present AE value of 9.38 eV is 170 meV higher than the calculated value for 5-ClU. A similar difference (120 meV) between calculated and experimental values of AEs was also observed in the case of uracil where the experimental value was 9.59 eV [11] and the calculated value 9.47 eV. Other experimental values for the AE of uracil given in [12] range from 9.45 to 9.68 eV. Also in the case of thymine, where the calculated AE was 9.02 eV, experimental determinations of the vertical ionization energy range from 9.02 to 9.2 eV [12,30]. From this, one may conclude that there is in general a small discrepancy between these calculations and the various experimental determinations.

Concerning the increased sensitivity of substituted pyrimidines to ionizing radiation, the present results can give an explanation why tissue modified with halouracils is more damaged in interaction with electrons. The AE of 5-ClU turns out to be slightly lower than the AE of regular uracil and therefore, damage caused by secondary electrons is possible at lower electron energies. Nevertheless, when the ratio of parent ion intensity and fragment ion intensities are compared in the mass spectra for uracil and 5-ClU, it turns out that the uracil molecule dissociates much stronger than the 5-ClU molecule. It should be also taken into account that the AEs of DNA bases (between 8 and 9 eV) [12] are lower than the AE of U and the ClUs. When positive and negative ion formation is considered, the increased radiosensitivity very likely will be due to the enhanced dissociative electron attachment cross section [13–17] for the halouracils leading to the destruction of the molecules and formation of genotoxic radicals.

Acknowledgements

This work has been supported by the FWF, and ÖNB, Wien, Austria and European Commission, Brussels.

References

[1] T.S. Lawrence, M.A. Davis, J. Maybaum, P.L. Stetson, W.D. Ensminger, Radiat. Res. 123 (1990) 192.
[2] S. Zamenhof, R. de Giovanni, S. Greer, Nature 181 (1958) 827.
[3] B.D. Michael, P.A. O'Neill, Science 287 (2000) 1603.

[4] C.M. DeLara, T.J. Jenner, K.M.S. Townsend, S.J. Marsden, P. O'Neill, Radiat. Res. 144 (1995) 43.
[5] M. Folkard, K.M. Prise, B. Brocklehurst, B.D. Michael, J. Phys. B At. Mol. Opt. Phys. 32 (1999) 2753.
[6] International Commission on Radiation Units and Measurements, ICRU Report 31, ICRU, Washington, DC, 1979.
[7] V. Cobut, Y. Fongillo, J.P. Patau, T. Goulet, M.-J. Fraser, J.-P. Jay-Gerin, Radiat. Phys. Chem. 51 (1998) 229.
[8] B. Boudaiffa, P. Cloutier, D. Hunting, M.A. Huels, L. Sanche, Science 287 (2000) 1658.
[9] G. Hanel, B. Gstir, S. Denifl, P. Scheier, M. Probst, B. Farizon, M. Farizon, E. Illenberger, T.D. Märk, Phys. Rev. Lett. 90 (2003) 1888104 (and references cited therein).
[10] S. Denifl, S. Ptasińska, M. Cingel, S. Matejcik, P. Scheier, T.D. Märk, Chem. Phys. Lett. 377 (2003) 74.
[11] B. Coupier, B. Farizon, M. Farizon, M.J. Gaillard, F. Gobet, N.V. de Castro Faria, G. Jalbert, S. Ouaskit, M. Carre, B. Gstir, G. Hanel, S. Denifl, L. Feketeova, P. Scheier, T.D. Märk, Eur. Phys. J. D. 20 (2002) 459.
[12] NIST chemistry web book, available at: http://webook.nist.gov.
[13] H. Abdoul-Carime, M.A. Huels, E. Illenberger, L. Sanche, J. Am. Chem. Soc. 123 (2001) 5354.
[14] H. Abdoul-Carime, M.A. Huels, F. Brüning, E. Illenberger, L Sanche, J. Chem. Phys. 113 (2000) 2517.
[15] H. Abdoul-Carime, M.A. Huels, E. Illenberger, L. Sanche, Int. J. Mass Spectrom. 228 (2003) 687.
[16] S. Denifl, S. Matejcik, B. Gstir, G. Hanel, M. Probst, P. Scheier, T.D. Märk, J. Chem. Phys. 118 (2003) 4107.
[17] S. Denifl, S. Ptasińska, S. Matejcik, E. Illenberger, P. Scheier, T.D. Märk, J. Chem. Phys., (2004) in press.
[18] S.D. Wetmore, R.J. Boyd, L.A. Eriksson, Chem. Phys. Lett. 343 (2001) 151.
[19] S.D. Wetmore, R.J. Boyd, L.A. Eriksson, Chem. Phys. Lett. 322 (2000) 129.
[20] D. Muigg, G. Denifl, A. Stamatovic, T.D. Märk, Chem. Phys. 239 (1998) 409.
[21] G. Denifl, D. Muigg, I.C. Walker, P. Cicman, S. Matejcik, J.D. Skalny, A. Stamatovic, T.D. Märk, Czech. J. Phys 49 (1999) 383.
[22] S. Matt, O. Echt, R. Wörgötter, V. Grill, P. Scheier, C. Liftshitz, T.D. Märk, Chem. Phys. Lett. 264 (1997) 149.
[23] G. Hanel, T. Fiegele, A. Stamatovic, T.D. Märk, Zeitschrift für Physikalische Chemie 214 (2000) 1137.
[24] T. Fiegele, G. Hanel, I. Torres, M. Lezius, T.D. Märk, J. Phys. B At. Mol Opt. Phys. 33 (2000) 4263.
[25] G. Hanel, J. Fedor, B. Gstir, M. Probst, P. Scheier, T.D. Märk, J. Phys. B At. Mol. Opt. Phys 35 (2002) 589.
[26] B. Gstir, G. Hanel, M. Probst, P. Scheier, N.J. Mason, T.D. Märk, J. Phys. B At. Mol. Opt. Phys 35 (2002) 1567.
[27] G. Hanel, B. Gstir, T. Fiegele, F. Hagelberg, K. Becker, P. Scheier, A. Snegursky, T.D. Märk, J. Chem. Phys. 116 (2002) 2456.
[28] M. Stano, S. Matejcik, J.D. Skalny, T.D. Märk, J. Phys. B 36 (2003) 261.
[29] P. Scheier, B. Dünser, R. Wörgötter, M. Lezius, R. Robl, T.D. Märk, Int. J. Mass Spectrom. Ion Proc. 138 (1994) 33.
[30] S.K. Kim, W. Lee, D.R. Herschbach, J. Phys. Chem. 100 (1996) 7933.